ORIGINAL PAPERS

Searching for antimicrobial photosensitizers among a panel of BODIPYs
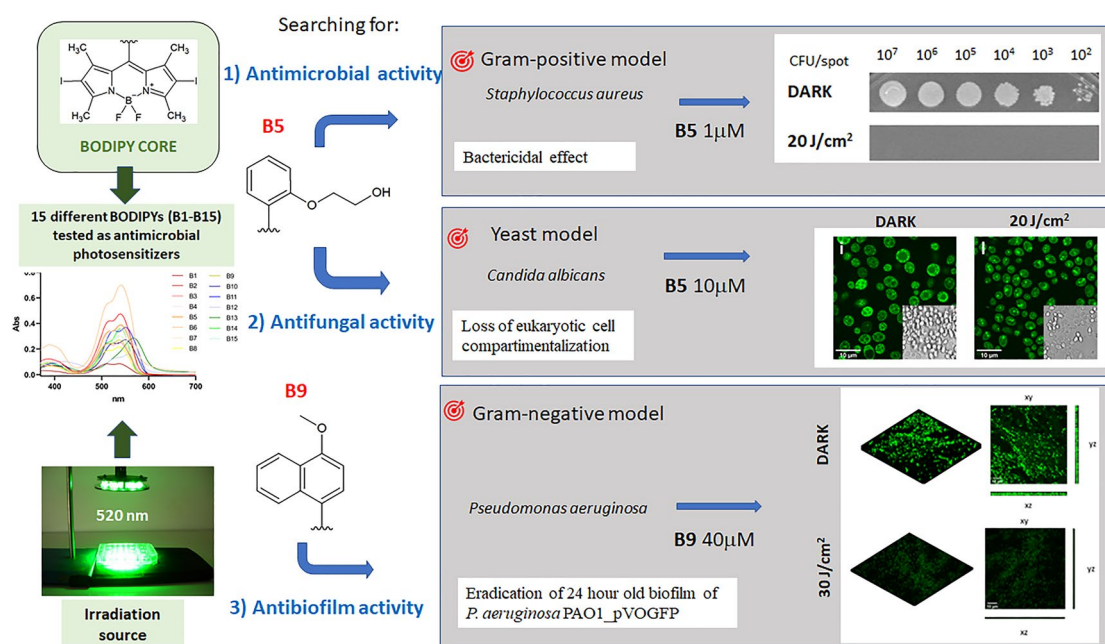
Viviana Teresa Orlandi[1] · Eleonora Martegani[1] · Fabrizio Bolognese[1] · Enrico Caruso[1]

Abstract

In recent years, antimicrobial Photodynamic Therapy (aPDT) gained increasing attention for its potential to inhibit the growth and spread of microorganisms, both as free-living cells and/or embedded in biofilm communities. In this *scenario*, compounds belonging to the family of boron-dipyrromethenes (BODIPYs) represent a very promising class of photosensitizers for applications in antimicrobial field. In this study, twelve non-ionic and three cationic BODIPYs were assayed for the inactivation of *Staphylococcus aureus*, *Pseudomonas aeruginosa* and *Candida albicans*. As expected, *S. aureus* showed to be very sensitive to BODIPYs and mild conditions were sufficient to reach good rates of photoinactivation with both neutral and monocationic ones. Surprisingly, one neutral compound (named **B9** in this study) resulted the best BODIPY to photoinactivate *P. aeruginosa* PAO1. The photoinactivation of *C. albicans* was reached with both neutral and mono-cationic BODIPYs. Furthermore, biofilms of the three model microorganisms were challenged with BODIPYs in light-based antimicrobial technique. *S. aureus* biofilms were successfully inhibited with milder conditions than those applied to *P. aeruginosa* and *C. albicans*. Notably, it was possible to eradicate 24-h-old biofilms of both *S. aureus* and *P. aeruginosa*. In conclusion, this study supports the potential of neutral BODIPYs as pan-antimicrobial PSs.

Graphical abstract

Extended author information available on the last page of the article

1 Introduction

In recent years, the increase of antimicrobial resistance in pathogens represents a threat to human health and modern society. As a result of intensive and sometimes excessive use of antibiotics and biocides, microorganisms have evolved resistance and/or tolerance mechanisms that rapidly spread in animals, the food chain, within the community and the healthcare setting [1, 2]. There is a great need to develop adjuvant strategies to overcome this issue [3]. Among these, Photodynamic Therapy (PDT) has initially been proposed as antitumoral approach and has recently been recommended in the antimicrobial field. Photo-oxidative stress, generated by photodynamic treatment, kills microorganisms, regardless of their drug susceptibility profile [4]. The photodynamic process exploits the power of visible light to activate a specific photosensitizer (PS) that undergoes chemico-physical reactions and generates highly reactive oxygen species (ROS) and/or singlet oxygen ($^1O_2$) in aerobic environments. If the PS is strictly associated with the microbial envelope and/or enters microbial cells, the arising oxidising species rapidly attack different cellular structures and macromolecules including lipids, proteins, and nucleic acids, leading to the death of microorganisms [5]. After a very fast and effective phototreatment, ROS riddle the bacteria at multiple sites in such a way that the overexpression of detoxifying enzymes (i.e. catalase, hydrogen peroxidase, heat shock proteins) does not provide a protective shield. However, the effectiveness of photodynamic treatment on bacteria without selection of resistant strains is still unverified, especially in sublethal-PDT conditions [6].

This technique showed to be efficient against many pathogens and could be easily exploited for clinical applications in the treatment of skin and oral cavity infections and as sanitizing approach [7].

Among antimicrobial PSs, there are several classes of natural or synthetic compounds: phenothiazinium salts, acridines, porphyrins, chlorins, phthalocyanines, fullerenes, curcumin, riboflavin, and xanthene [4]. In 2005, Gallagher et al. identified boron-dipyrromethenes (BODIPYs) as a class of chemicals with suitable features for anticancer PDT. In particular, cationic BODIPYs were further highlighted as promising PSs to kill bacteria and fungi [8–10]. BODIPYs have a typical skeleton based on difluoro-boradiazaindacene, whose synthetic pathway is relatively flexible and easy, starting from commercial pyrroles and acid chlorides, anhydrides, aldehydes, or ketones. The core of BODIPY presents a great reactivity and chemical versatility that allows the incorporation of different functional groups and the generation of new compounds with diverse properties [11]. Even if BODIPY dyes are excited by light around 500 nm, new compounds absorbing at longer wavelengths could be developed by appropriate chemical modifications [12]. Usually, BODIPYs are widely applied as fluorophores to label biomolecules (e.g. fatty acids, nucleotides, proteins, etc.), detect ionic species, and as light-harvesting antennas to improve the absorption of different chromophores [13, 14]. However, fluorescence emission could be detrimental in PDT application. At this aim, the iodination of BODIPYs converts the highly fluorescent molecule into a potent PS, causing a bathochromic shift of maximum absorption peak in ∼ 30 nm, decreasing fluorescence properties, and improving singlet oxygen generation [12, 15].

If BODIPYs have been investigated and properly designed as antitumoral photosensitizers [11], Durantini et al. recently reported that only a dozen of BODIPYs with different chemical complexity and charge have been investigated in the antimicrobial field [16]. Furthermore, in the design and discovery of new materials, formulations containing BODIPYs have been proposed. For example, BODIPYs were used for surface coating or were included in copolymers, nanofibers and glycomimetic compounds [17–21].

In this work, a panel of 15 BODIPYs was investigated for the antimicrobial photodynamic activity. All compounds are characterised by a 4,4-difluoro-1,3,5,7-tetramethyl-4-bora-3a,4a-diaza-s-incacene core, modified by the insertion of two iodine atoms in positions 2 and 6 by electrophilic aromatic substitution. BODIPYs differ from each other for the substituent in the meso-position (position 8), which can be an aromatic ring with an activating or deactivating substituent, holding non-ionic groups or positive charges [10, 22–25]. Since neutral compounds, belonging to different photosensitizer families, showed to be selectively active against Gram-positive bacteria [26], BODIPYs were tested against *S. aureus*. This screening was extended to the Gram-negative bacterium *Pseudomonas aeruginosa* and to the yeast *Candida albicans*. Active PSs were furtherly assayed for the inhibition and/or eradication of microbial biofilms, the most difficult goal in antimicrobial field.

2 Materials and methods

2.1 Photosensitizers

A panel of 15 borondipyrromethens (BODIPYs) was employed in this study (Table 1). Compounds **B1**–**B9** are

characterised by an alkyloxy group on the phenyl ring in 8 position of the BODIPY core, **B10**–**B12** bear halogen atoms on the phenyl ring, and **B13**-**B15** are positively charged. PSs were synthetized as previously described [10, 22–25], were dissolved in DMSO at a final concentration of 1 mM, and stored at 4 °C until needed. Compounds **B14** and **B15** were synthetized as follows:

4,**4-difluoro-2**,**6-Diiodo-1**,**3**,**5**,**7-tetramethyl-8-(4-(4-bromopyridiniobuthoxy)phenyl)-4-bora-3a**,**4adiaza-s-indacene** (**B14**). A solution of 70 mg (0.098 mmol) of B7 in 4 mL of freshly distilled pyridine was kept to 80 °C for 3 days. The solution was neutralized with HCl 1 M, the formed precipitate was recovered by centrifugation (5000 rpm for 15 min) and thoroughly washed with diethyl ether. 24 mg (yield: 30.6%). $C_{28}H_{29}BBrF_2I_2N_3O$, Mw = 806.1. UV–vis(DMSO): 534 nm ($\varepsilon = 73,900$). LogP = 0.44[27]. $^1O_2 = 0.8$[10]. ^1H NMR (DMSO) δ: 1.39 (s, 6H, $2xCH_3$); 1.80 (t, 2H, CH_2); 2.14 (t, 2H, CH_2); 2.54 (s, 6H, $2xCH_3$); 4.10 (t, 2H, CH_2N); 4.73 (t, 2H, CH_2O); 7.13 (d, 2H); 7.30 (d, 2H); 8.20 (t, 2H); 8.63 (t, 1H); 9.16 (d, 2H). ^{13}C NMR (DMSO) δ: 15.14; 16.21; 26.75; 28.98; 32.12; 66.47; 85.30; 113.91; 120.31; 129.23; 130.61; 133.16; 139.73; 143.12; 144.78; 147.65; 156.21; 157.98.

MS–ESI$^+$: m/z 726.01 (M—Br) (100%). **4**,**4-difluoro-2**,**6-Diiodo-1**,**3**,**5**,**7-tetramethyl-8-(4-(4-bromopyridiniooctanoxy)phenyl) -4-bora-3a**,**4adiaza-s-indacene** (**B15**). 98 mg (0.125 mmol) of B8 in 6 mL of pyridine was reacted as described for compound B14. 31 mg (yield: 29.6%). $C_{32}H_{37}BBrF_2I_2N_3O$ M.W.: 862.2 g/mol. UV–VIS (DMSO): 534 nm ($\varepsilon = 60,500$). LogP = 1.23. $1O2 = 0.6$. ^1H NMR (DMSO) δ: 1.35–1.43 (m, 8H, $4xCH_2$); 1.40 (s, 6H, $2xCH_3$); 1.75 (t, 2H, CH_2); 1.94 (t, 2H, CH_2); 2.54 (s, 6H, $2xCH_3$); 4.04 (t, 2H, CH_2N); 4.63 (t, 2H, CH_2O); 7.11 (d, 2H); 7.28 (d, 2H); 8.18 (t, 2H); 8.62 (t, 1H); 9.13 (t, 2H). ^{13}C NMR (DMSO) δ: 12.13; 14.57; 25.97; 26.14; 28.08; 28.68; 29.22; 32.77; 33.93; 68.09; 86.35; 115.20; 121.07; 126.89; 129.18; 131.89; 141.98; 142.53; 143.17; 148.40; 155.23; 159.70. MS–ESI$^+$: m/z 782.4 (M—Br) (100%).

2.2 Microbial strains and culture conditions

Staphylococcus aureus strains ATCC 6538P (methicillin sensitive) and ATCC 43300 (methicillin resistant) used in this study were grown in Tryptic Soy Broth (TSB) medium. In addition to the model strain *Pseudomonas aeruginosa* PAO1 [27] and its isogenic derivative expressing Green-Fluorescent protein [28, 29], the clinical isolates UR48 and BT1 from patients with catheter-associated urinary tract infection and cystic fibrosis, respectively, were investigated [30, 31]. For the maintenance of *P. aeruginosa* strains, Luria Bertani (LB) medium was used. *Candida albicans* ATCC 14053 and clinical strains Ca1 and Ca2 recovered from patients with

urinary tract infections [32] were grown in YPD medium (Yeast extract 10 g/L, Peptone 20 g/L, and L-Dextrose 20 g/L). All microbial strains were grown overnight at 37 °C on solid media (15 g/l agar) or in liquid media on an orbital shaker at 200 rpm.

2.3 Light sources

The lighting unit employed for the photoactivation of BODIPYs is a Light Emitting Diode (LED) apparatus with 12 diodes distributed on a 11 cm-diameter disk equipped with a heat sinker. LEDs have a maximum emission peak at 520 nm, suitable for the activation of BODIPYs. The system is powered by a 50 W current transformer and the lamp was positioned at 35 cm over the samples with a fluence rate of 2.4 mW/cm^2.
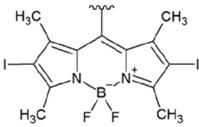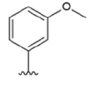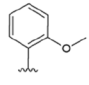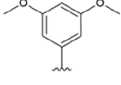
2.4 Binding assay
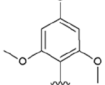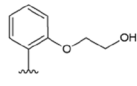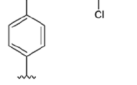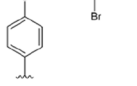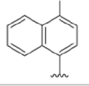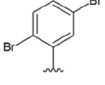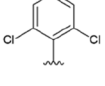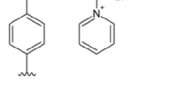
BODIPYs were tested for their interaction with bacterial and yeast cells [29]. Upon overnight growth of microbial strains (*S. aureus* ATCC 6538P, *P. aeruginosa* PAO1, *C. albicans* ATCC 14053), cell cultures were centrifuged at 5000 rpm for 10 min. Pellets were tenfold diluted in sterile water and 10 μM BODIPYs were added to the cell suspensions. Untreated cells and cells added with DMSO 4% (V/V) were included as controls. Samples were incubated in the dark at 37 °C for 1 h to allow the interaction between cells and PSs. After centrifugation at 10,000 rpm for 5 min, the visible spectra of the supernatants were recorded (k = 380–700 nm). A calibration plot (μM concentration *vs* OD$_x$) was obtained for each PS and used to calculate the amount of free or bound PS. Data were calculated as % mean ± standard deviation of at least three independent experiments.

2.5 Photoinactivation assay

2.5.1 Photo-spot test

The photo-spot test, previously optimized for *P. aeruginosa* [33], was adapted to *S. aureus* and *C. albicans* as follows: overnight cultures of *S. aureus* ATCC 6538P and *P. aeruginosa* PAO1 were centrifuged (4000 rpm for 10 min) and suspended in phosphate buffer saline (PBS, KH_2PO_4/K_2HPO_4 10 mM, pH 7.4) at final concentrations of ~ $10^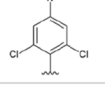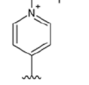9$, 10^8, 10^7, 10^6, 10^5, 10^4 CFU/mL in 96-well plates. Similarly, overnight cultures of *C. albicans* ATCC 14053 were diluted in PBS at ~ 10^8, 10^7, 10^6, 10^5, 10^4, 10^3 CFU/mL. PSs were added in 96-well plates to 100 μl of microbial samples at a final concentration of 1 μM for *S. aureus* and 10 μM for *P. aeruginosa* and *C. albicans*, respectively. Untreated and DMSO treated samples were included as controls.

Table 1 BODIPYs used in this study

BODIPY core		PS	Substituents	Chemical denomination	Ref
	Activated aromatic ring	B1		4,4-Difluoro-2,6-Diiodo-1,3,5,7-Tetramethyl-8-(3′-Methoxyphenyl) -4-Bora-3a,4adiaza-s-Indacene	[22]
		B2		4,4-Difluoro-2,6-Diiodo-1,3,5,7-Tetramethyl-8-(2′-Methoxyphenyl) -4-Bora-3a,4adiaza-s-Indacene	[23]
		B3		4,4-Difluoro-2,6-Diiodo-1,3,5,7-Tetramethyl-8-(3′,5′-Dimethoxyphenyl)-4-Bora-3a,4adiaza-s-Indacene	[23]
		B4		.4,4-Difluoro-2,6-Diiodo-1,3,5,7-Tetramethyl-8-(2′,4′,6′-Trimethoxyphenyl)-4-Bora-3a,4adiaza-s-Indacene	[23]
		B5		4,4-Difluoro2,6-Diiodo-1,3,5,7-Tetramethyl-8-[2′-(2″-Hydroxyethoxy)Phenyl)]-4-Bora-3a,4adiaza-s-Indacene	[23]
		B6		4,4-Difluoro-2,6-Diiodo-1,3,5,7-Tetramethyl-8-[4′-(4″-Chlorobuthoxy)Phenyl)]-4-Bora-3a,4adiaza-s-Indacene	[23]
		B7		4,4-Difluoro-2,6-Diiodo-1,3,5,7-Tetramethyl-8-{4-[(4-Bromobutyl) oxy]phenyl}-4-Bora-3a,4adiaza-s-Indacene	[24]
		B8		4,4-Difluoro-2,6-Diiodo-1,3,5,7-Tetramethyl-8-{4-[(4-Bromooctyl) oxy]phenyl}-4-Bora-3a,4adiaza-s-Indacene	[25]
		B9		4,4-Difluoro-2,6-Diiodo-1,3,5,7-Tetramethyl-8-(4′-Methoxynaphthalene)-4-Bora-3a,4a-diaza-s-Indacene	[22]
	Deactivated aromatic ring	B10		4,4-Difluoro-2,6-Diiodo-1,3,5,7-Tetramethyl-8-(2′,5′-Dibromophenyl)-4-Bora-3a,4a-diaza-s-Indacene	[23]
		B11		4,4-Difluoro-2,6-Diiodo-1,3,5,7-Tetramethyl-8-(2′,6′-Dichlorophenyl)-4-Bora-3a,4a-diaza-s-Indacene	[22]
		B12		4,4-Difluoro-2,6-Diiodo-1,3,5,7-Tetramethyl-8-(2′,6′-Dichloro-4′-Nitrophenyl)-4-Bora-3a,4adiaza-s-Indacene	[23]
	Monocationic	B13		4,4-Difluoro-2,6-Diiodo-1,3,5,7-Tetramethyl-8-(N-methyl-4-Pyridyl)-4-Bora-3a,4adiaza-s-Indacene	[10]
		B14		4,4-Difluoro-2,6-Diiodio-1,3,5,7-Tetrametil-8-(4-(4-pyridinobutoxy)phenyl)-4-Bora-3a,4adiaza-s-Indacene	This study
		B15		4,4-Difluoro-2,6-Diiodio-1,3,5,7-Tetrametil-8-(4-(4-pyridinooctanoxy)phenyl)-4-Bora-3a,4adiaza-s-Indacene	This study

To evaluate intrinsic toxicity, microbial samples were incubated in the dark with BODIPYs for 10 min, 1 h or 6 h, respectively. A volume of 5 µl of each suspension was spotted on LB agar plates that were incubated overnight at 37 °C. The intrinsic toxicity was evaluated by comparing the growth of corresponding dilutions between treated and untreated samples. The absence of each microbial spot from the highest dilutions in treated samples was calculated as 1 (or more) Log unit decrease in cell viability: higher Log values are associated with higher rates of intrinsic toxicity.

PS photoactivity was assayed after 1 h of dark incubation. Microbial cells were prepared as previously described, spotted on LB agar plates and irradiated under light at 520 nm (20 J/cm^2, 138 min) to activate PSs; dark incubated controls were included. After overnight incubation at 37 °C, the growth spots were compared to untreated and dark incubated cells: higher Log unit decrease was associated with higher photo-antimicrobial activity. Spot-tests and photo-spot tests were performed at least in triplicate.

2.6 Photoinactivation of suspended cultures

Overnight cultures of *S. aureus* ATCC6538P, *P. aeruginosa* PAO1, and *C. albicans* ATCC14053 were diluted to suitable concentrations in PBS in 12-well plates. BODIPYs were added to 1 mL of cellular suspensions at a final concentration of 1 µM for *S. aureus* and 10 µM for *P. aeruginosa* and *C. albicans,* respectively. Untreated cells and DMSO-treated cells were included as controls. After 1 h dark incubation, cells were irradiated at 520 nm (20 J/cm^2, 138 min) or kept in the dark. Cell viability was checked by plating 10 µl samples deriving from tenfold serial dilutions of treated and untreated cells and expressed as CFU/mL. Photoinactivation experiments were performed at least in triplicate for each strain and chosen BODIPYs.

2.7 Photodynamic treatment of microbial biofilms

2.7.1 Inhibition of biofilm formation

S. aureus ATCC 6538P and ATCC 43300 and *P. aeruginosa* strains (PAO1, UR48, BT1) were grown at 37 °C in minimal medium supplemented with 10 mM glucose and 0.2% W/V casamino acids as carbon sources. Overnight cultures were diluted in fresh medium in 24-well plates at a concentration of 10^7 CFU/mL. BODIPYs were added at a final concentration of 0.5 µM for *S. aureus* strains and 40 µM for *P. aeruginosa* strains, respectively. After 1 h of dark incubation, *S. aureus* was irradiated under 520 nm light at 20 J/cm^2 (138 min) and *P. aeruginosa* at 30 J/cm^2 (207 min). The following control samples were included: + PS− light, − PS + light, − PS− light, + DMSO−light, + DMSO + light. Biofilms were allowed to form at 37 °C for 24 h. Overnight cultures of *C. albicans* ATCC 14053 and clinical strains (Ca1, Ca2) were 100-fold diluted in sterile water and incubated for 1 h in the dark at 37 °C with 20 µM BODIPYs. After irradiation under light at 520 nm (30 J/cm^2, 207 min), 250 µL of YPD medium were added and samples were incubated at 37 °C for 24 h to allow biofilm formation. Control samples were included as previously described.

2.8 Eradication of 24-h-old biofilms

Bacterial strains and *C. albicans* were grown overnight at 37 °C in minimal medium (M9 added with glucose and CAA) and YPD medium, respectively. Suspensions were diluted in fresh medium to reach a cellular concentration of ~10^7 CFU/mL and the biofilm was let to form for 24 h at 37 °C. BODIPYs at 40 µM (*P. aeruginosa*) or 0.5 µM (*S. aureus*) concentrations were added to 24-h-old biofilms. To rule out YPD interference in *C. albicans,* planktonic phase was removed and replaced with PBS added with BODIPYs 40 µM. After one-hour dark incubation, each biofilm was irradiated under light at 520 nm at 30 J/cm^2 (207 min) for *P. aeruginosa* and *C. albicans* and 20 J/cm^2 (138 min) for *S. aureus*, respectively. A control panel as described previously was included for each experiment.

2.8.1 Biofilm evaluation

Planktonic phases were collected and adherent cells were recovered by scraping and suspended in 1 mL of PBS.

Cell viability of both phases was determined and expressed as CFU/mL and as CFU/well, respectively. Corresponding replicates were stained with crystal violet (CV) for total adherent biomass quantification, after planktonic biomass removal. Briefly, plates were washed with 1 mL PBS, and biofilms were treated with one millilitre of CV 0.1% W/V for 20 min. CV was removed and each well was gently washed with 1 mL PBS. The remaining CV, which indicated the amount of biofilm, was dissolved in acetic acid 30% V/V. The amount of solubilized dye was spectrophotometrically measured at 590 nm. If necessary (OD > 1), suitable dilutions were used and the OD value was determined proportionally. Experiments were performed in triplicate.

2.9 Confocal laser scanning microscopy analyses

Confocal microscopy analyses were performed to compare the effect of PDT treatment with BODIPYs on *C. albicans* cells. After treatment as detailed in paragraph 2.5, *C. albicans* ATCC 14053 cells were centrifuged (10,000 rpm, 5 min) and pellets were suspended in PBS to a final concentration of 10^6 CFU/mL. The fluorescent BODIPY dye (4,4-difluoro-1,3,5,7-tetramethyl-8-(2-methoxyphenyl)-4-bora-3a,4a-diaza-s-indacene) was added to a final

concentration of 2 μM [32] and cells were incubated for 30 min at 37 °C on a shaker at 50 rpm. Samples were centrifuged (10,000 rpm, 10 min) and pellets suspended in 20 μL of PBS. All microscope analyses were performed on a Leica TCS SP5 confocal laser scanning microscope (CLSM; Leica Microsystems, Wetzlar, Germany) with 488 nm laser excitation. Images were recorded using a 63 × objective lens.

In a similar way, PAO1_pVOGFP strain, which expresses GFP recombinant protein under the control of pBAD arabinose inducible promoter, was used to assay the anti-biofilm activity of **B9** compound [29]. Overnight cultures of PAO1_pVOGFP in minimal medium were diluted at a final concentration of 10^7 CFU/mL in fresh medium and added to coverslip glasses positioned in 35 mm Petri dishes. BODIPY **B9** was added at a final concentration of 40 μM. Samples were dark incubated for 1 h and irradiated under 520 nm light at 30 J/cm^2 (207 min); control samples -PS-L, -PS + L, + DMSO-L, + DMSO + L, + PS-L, were also included. Biofilms were allowed to form at 37 °C for 24 h in humidified chambers. Planktonic phases were removed and GFP expression was induced by the addition of arabinose 0.1% W/V for 1 h. Images were obtained using a 63 × objective lens. Simulated 3D images of *P. aeruginosa* biofilms were generated using the free open-source software ImageJ (National Institute of Health, USA).

2.10 Statistical analyses

Photoinactivation experiments on suspended cells and biofilms were performed at least in triplicate with microbial cultures. Statistical analyses were assessed by one-way ANOVA analysis.

3 Results

3.1 Intrinsic toxicity and degree of binding of BODIPYs

The BODIPYs considered in this study share a phenyl group in *meso*-position, carrying different substituents (Table 1). Among non-ionic molecules, **B1**–**B9** have activating groups, while **B10**–**B12** carry deactivating substituents on the benzyl group; **B13**–**B15** are mono-cationic compounds. Methoxy groups are present in position 3′ and 2′ for **B1** and **B2**, while in position 3′, 5′ in **B3**, and 2′,4′,6′ in compound **B4**, respectively. Compound **B5** bears a 2″-hydroxy ethoxy group in position 2'. Compound **B6** carries a 4′-chlorobutoxy group in position 4, **B7** carries the same alkyloxy chain with bromine at the end of the carbon chain. **B8** is similar to compound **B7** but has a C8 chain instead of C4 chain, and **B9** presents a 4′-methoxynaphtalene in *meso*-position. PSs with

deactivating groups on the aromatic ring are characterized by bromine atoms in 2′,5′ positions (**B10**) or chlorin atoms in 2′, 6′ positions (**B11**). Compound **B12** differs from **B11** only for the presence of a *nitro*-group in 4′ position. Mono-cationic BODIPYs carry a pyridyl group that confers a positive charge. **B13** bears a N-methyl-4′-pyridiyl substituent in *meso*-position and has been previously tested for antimicrobial activity [10, 34, 35]. In **B14** and **B15** the pyridyl group is positioned at the end of a C4 (**B14**) or C8 (**B15**) alkyloxy chain and have been tested for the first time in this study. The absorption spectra of the described BODIPYs are shown in Fig. 1.

As detailed in Fig. 2, the neutral compounds show a preferential binding for the Gram-positive bacterium *S. aureus* with yield values higher than 60%, while binding degrees lower than 40% were observed in *P. aeruginosa* and *C. albicans*. Taken together, these data show that the three mono-cationic BODIPYs interact with microorganisms regardless of their cell-wall organization.

Compounds with proven dark toxicity were excluded from further assays as the PDT killing should be the result of specific irradiation. This underscores the potential added-value of photodynamic approach as "on demand" antimicrobial strategy. *S. aureus* showed dark sensitivity to 1 μM concentration of the neutral compound **B9** and the cationic compound **B14**, while *P. aeruginosa* was almost insensitive to 10 μM concentration of non-ionic BODIPYs and sensitive to 10 μM concentration of cationic BODIPYs **B13** and **B14**. The yeast showed a sensitivity pattern more similar to the Gram-negative strain: most neutral BODIPYs did not display any intrinsic toxicity, while mono-cationic molecules were toxic to *C. albicans*. As further detailed in Table 2, PS toxicity profiles were dose, time and strain dependent.

3.2 Photodynamic activity of BODIPYs

As putative PSs should be active only upon irradiation, compounds without any intrinsic toxicity were further investigated for their photoactivity (Table 3). In particular, *S. aureus* showed a high sensitivity to most BODIPYs at 1 μM concentration. Among the neutral compounds, **B5** showed the highest anti-*Staphylococcal* activity, inhibiting the growth of the sample up to 10^7 CFU/spot. **B13** and **B15** compounds, both mono-cationic, showed ~ 4 Log$_{10}$ unit difference in antimicrobial activity. In *P. aeruginosa* PAO1, unexpectedly, several non-ionic BODIPYs, upon activation, inhibited the growth more efficiently than the cationic ones: for example, the neutral **B2** caused a ~ 5.7 Log unit reduction, while the cationic **B15** ~ 2.6 Log units, respectively. *C. albicans* was sensitive to both neutral and monocationic BODIPYs.
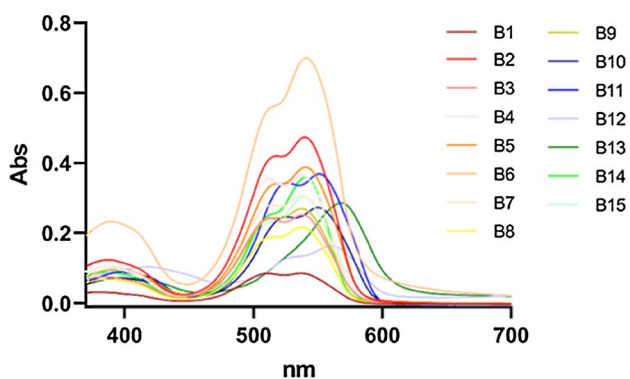
Fig. 1 Visible light absorption spectra of BODIPYs (**B1-B15**)

In order to evaluate the efficacy of BODIPYs in killing suspended cultures of different microorganisms, PSs with the highest rates of photoinactivation were tested against *S. aureus*, *P. aeruginosa* and *C. albicans*, respectively. The two bacterial species showed different sensitivities to aPDT. In the Gram-positive microorganism, all the chosen compounds were active at 1 μM concentration and, among these, non-ionic **B2** and **B5** caused the highest viability reduction (~ 6 Log units) reaching the detection limit of the system (10^2 CFU/mL) (Fig. 3a). On the other hand, *P. aeruginosa* was particularly tolerant to the chosen BODIPYs at 10 μM concentration, and only the neutral **B9** was photoactive (Fig. 3b).

Fig. 2 Binding degrees of BODIPYs (**B1-B15**) in *S. aureus* ATCC 6538P (**a**), *P. aeruginosa* PAO1 (**b**), and *C. albicans* ATCC 14053 (**c**). Values are presented as % of PSs (mean ± standard deviation) bound to cells upon one hour of dark incubation. BODIPYs were administered to cells at a concentration of 10 μM and experiments were independently repeated at least three times
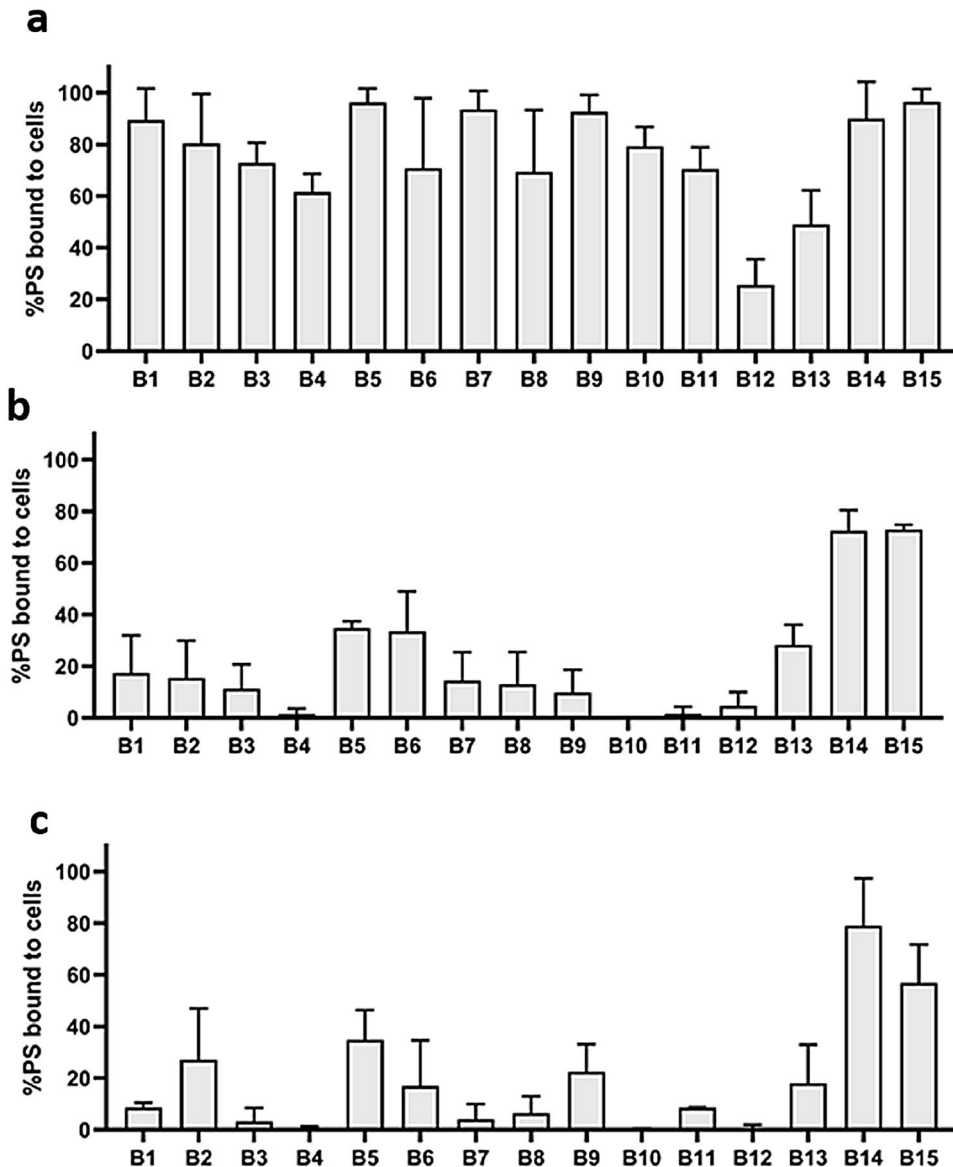
Given that both non-ionic and cationic BODIPYs showed similar activities against *C. albicans* (Fig. 3c), we performed a confocal microscopy analysis aimed at highlighting possible differential effects at the morphological level. Control samples (− PS − Light, − PS + Light, + DMSO − Light, + DMSO + Light) displayed the expected compartmentalization with a dark nucleus, not permeable to the chosen fluorophore. After PDT treatment with all tested BODIPYs, no organelles were recognizable and a foggy signal of the fluorescent probe was equally distributed in all the cell volume, and a peculiar accumulation of the tracer was clearly visible in a central region of the cytoplasm (Fig. 4). This could be ascribable to a different probe distribution related to a change in cellular anatomy. Namely, cells were egg-shaped with inherent volume reduction if compared to control samples. This evident alteration of cell structure was concomitant with loss of cell viability. The experimental outcome was common to all photosensitizers and all candidates were further used for biofilm photoinactivation.

3.2.1 Photodynamic treatment of *S. aureus* biofilms

Compounds **B2** and **B5** were active in inhibiting the formation of *S. aureus* biofilms at 0.5 μM concentration. As detailed in Fig. 5, DMSO and DMSO solubilized PSs in the dark were ineffective, while photoactivated BODIPYs impaired significantly the formation of biofilms. Cells exposed to photooxidative stress were not able to form biofilms comparable to those of untreated samples: the observed impairments were statistically significant for both adherent and planktonic subpopulations. As similar results were observed for MRSA strain, PDT treatment could be exploited as a promising tool in clinical applications.

As the eradication of formed biofilms represents a main issue in this field, 24-h-old MSSA biofilms were incubated one hour in the dark with 0.5 μM PSs and irradiated at a fluence of 20 J/cm^2. Although no change was observed in total adherent biomass, cellular viability of planktonic and sessile populations was reduced of 5 log units (Fig. S1).

Table 2 Intrinsic toxicities of BODIPYs (**B1**-**B15**). *S. aureus* ATCC 6538P and *P. aeruginosa* PAO1 cells were spotted on LB agar from 10^7 up 10^2 CFU/spot, *C. albicans* ATCC 14053 cells from 10^6 up 10 CFU/spot

PS		*S. aureus* PS [1 μM]				*P. aeruginosa* PS [10 μM]				*C. albicans* PS [10 μM]			
		Log$_{10}$ reduction			Spot test images (6 h incubation)	Log$_{10}$ reduction			Spot test images (6 h incubation)	Log$_{10}$ reduction			Spot test images (6 h incubation)
Incubation time		10'	1 h	6 h	CFU/spot 10^7 10^6 10^5 10^4 10^3 10^2	10'	1 h	6 h	CFU/spot 10^7 10^6 10^5 10^4 10^3 10^2	10'	1 h	6 h	CFU/spot 10^6 10^5 10^4 10^3 10^2 10
Untreated		0	0	0		0	0	0		0	0	0	
Solvent ctrl		0	0	0		0	0	0		0	0	0	
Activated aromatic ring	**B1**	0	0.6	2.5		0	0	0		0	0.3	1.5	
	B2	0	0	0		0	0	0		0	0	1	
	B3	0	0	0		0	0	0		0	0	0	
	B4	0	0	0		0	0	0		0	0	0	
	B5	0	0	1.3		0	0	0		0	0	0	
	B6	0	0	0		0	0	0		0	0	0	
	B7	0	0.6	2.3		0	0	0		0	0	0	
	B8	0	0	2		0	0	0		0	0	0	
	B9	2	3	4		0	0	0		0	1.6	2	
Deactivated aromatic ring	**B10**	0	0	0		0	0	0		0	0	0	
	B11	0	0	0		0	0	0		0	0	0	
	B12	0.5	0.5	1.3		0	0	0		0	0	0	
Monocationic	**B13**	0	0	0		0.6	0.6	3		0	0	1	
	B14	1.3	2	2.3		0	0	1.6		1.3	3	3.3	
	B15	0	0	0		0	0	0		0	0	2	

BODIPYs were administered at 1 μM to *S. aureus* cells and 10 μM to *P. aeruginosa* and *C. albicans* and incubated in the dark 10 min, 1 h, 6 h. Untreated and solvent-treated (solvent ctrl) samples were also included in the figure as controls. After overnight incubation at 37 °C, Log$_{10}$ reduction unit were reported as the average of at least three independent experiments. For each strain, the growth spot test images upon 6 h of dark incubation are shown as representative.

Table 3 Photodynamic activities of BODIPYs on *S. aureus* ATCC 6538P, *P. aeruginosa* PAO1, *C. albicans* ATCC 14053 cells evaluated by photo-spot test

S. aureus			*P. aeruginosa*			*C. albicans*		
PS [1 µM] Green light 520 nm	Log_{10} reduction 20 J/cm^2	Photo-spot test images CFU/spot	PS [10 µM] Green light 520 nm	Log_{10} reduction 20 J/cm^2	Photo-spot test images CFU/spot	PS [10 µM] Green light 520 nm	Log_{10} reduction 20 J/cm^2	Photo-spot test images CFU/spot
Untreated	0		Untreated	0		Untreated	0	
Solvent ctrl	0		Solvent ctrl	0		Solvent ctrl	0	
B2	5.3		B1	0		B2	5	
B3	4.5		B2	5,7		B3	1	
B4	4		B3	0		B4	1	
B5	7		B4	0		B5	5	
B6	5.3		B5	4.3		B6	1	
B10	6		B6	0		B7	6.3	
B11	5.6		B7	1		B8	3.3	
B13	1.3		B8	0		B10	2	
B15	5.3		B9	4.3		B11	0	
			B10	0		B12	3.3	
			B11	0		B13	4.6	
			B12	0				
			B15	2.6				

BODIPYs (**B1**-**B15**) were administered at a concentration of 1 µM to *S. aureus* and 10 µM to *P. aeruginosa* and *C. albicans* and incubated in the dark for one hour. Microbial diluted samples were spotted on agar plates and irradiated under 520 nm light (20 J/cm^2). After irradiation, cells were incubated overnight at 37 °C. Untreated and solvent-treated (solvent ctrl) samples were also included in the figure as controls. Log_{10} reduction unit was reported as the average of at least three independent experiments. For each strain, one image representative of photo-spot test is shown

3.2.2 Photodynamic treatment of *P. aeruginosa* biofilms

As the neutral compound **B9** showed good activity against the model organism *P. aeruginosa* PAO1, it was used in anti-biofilm experiments with two different clinical isolates: UR48 from a patient with CAUTI (catheter associated urinary tract infection) and BT1 from a patient with CF (Cystic Fibrosis) [30, 31]. Given that Crystal Violet staining is unable to discriminate between matrix and cellular components of adherent microbial communities, OD_{590} values are still useful to quantify the overall biofilm formation in different experimental conditions (Fig. 6). Accordingly, we observed that PAO1, UR48 and BT1 strains showed average OD_{590} values of ~ 6, 10 and 22, respectively. An average reduction of ~ 90% in OD_{590} was observed for all *P. aeruginosa* strains upon increasing **B9** concentration from 10 to 40 µM and fluence rate from 20 to 30 J/cm^2. The administration of DMSO alone caused an increase of OD_{590} in PAO1 and UR48 strains, but not in BT1. PDT with BODIPY **B9** reduced cell viability of at least 5 Log units for both adherent and planktonic populations of all tested strains.
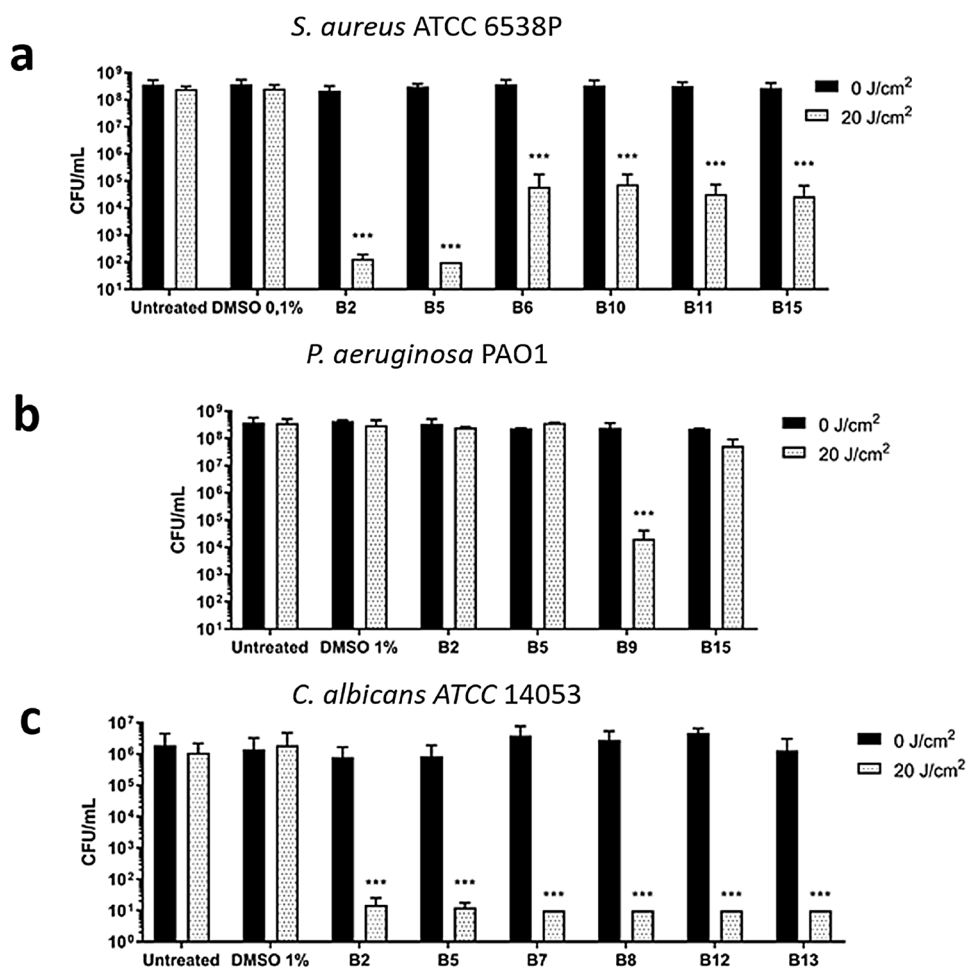
The potential of compound **B9** in eradicating structured biofilms was investigated in the model strain PAO1. The treatment did not alter the amount of the adherent biomass, but compromised significantly the viability of sessile and suspended cells (Fig. S2). Morphological studies were performed on PAO1-pVOGFP [28, 29] by confocal microscopy analysis. The photo-treatment with **B9** caused a decrease of fluorescence and biofilm thickness (Fig. 7). These effects could be ascribable to an impairment in cell physiology, including a possible effect on recombinant protein function and is consistent with the decrease in cell viability previously reported [36]. This outcome suggests that most of the cells were damaged immediately after PDT treatment, and they could be possibly more susceptible to antibiotic or biocide administration. Even if no biofilm destruction could be promptly achieved, a significant anti-biofilm effect on viable components of biofilm was obtained.

3.2.3 Photodynamic treatment of *C. albicans* biofilms

Non-ionic compounds **B2**, **B5**, **B7**, **B8**, **B12** and mono-cationic **B13** BODIPYs were assessed for their inhibitory effect on biofilm formation of the model yeast *C. albicans* ATCC 14053 (Fig. 8). None of the PSs showed significant dark toxicity, while photodynamic treatment caused a significant reduction (~50%) in biofilm formation. Among PSs, the non-ionic **B7** and the mono-cationic **B13** showed the

Fig. 3 Photodynamic inactivation of suspended cells of *S. aureus* ATCC 6538P (**a**), *P. aeruginosa* PAO1 (**b**), and *C. albicans* ATCC 14053 (**c**). The chosen BODIPYs were administered at 1 µM concentration to *S. aureus* cells (10^8 CFU/ml), and 10 µM to *P. aeruginosa* (10^8 CFU/ml) and *C. albicans* (10^6 CFU/ml) samples and dark incubated for one hour. Cells were irradiated by light at 520 nm (20 J/cm^2) or dark incubated. Untreated and DMSO-treated samples were included as controls for each pathogen. After irradiation, the cellular viability was checked. Dark controls are represented as black bars, while irradiated samples as dotted bars. Viability yields are expressed as CFU/mL (mean ± standard deviation). The experiments have been performed at least three times and statistical analyses were performed by one-way ANOVA (***$p < 0.0001$)

4 Discussion

In this study we tried to search for new antimicrobial PSs among a panel of neutral and cationic BODIPYs. It is known that cationic compounds are more prone than neutral ones to interact with negative charged components of both bacterial and yeast envelopes. In particular, teichoic acids/lipoteichoic acids on the mureinic layer on Gram-positive bacteria and lipopolysaccharides on the outer membrane of Gram-negative bacteria favour electrostatic interactions with cationic photosensitizers. Similarly, in yeast cells, the robust polysaccharide skeleton linked to chitin and to highly glycosylated mannoproteins confers the anionic charge responsible for interaction with cationic PSs [37]. As expected, the tested

highest antimicrobial activities against both adherent and planktonic subpopulations. These PSs showed to be efficient also in inhibiting the biofilm formation of the clinical strains Ca1 and Ca2 (Fig. S3). Differently from *S. aureus* and *P. aeruginosa* PAO1, *C. albicans* ATCC 14053 24-h-old biofilms were not eradicated by **B13** (Fig. S4).

cationic BODIPYs showed higher extent of binding than neutral ones, regardless of microbial cell wall structure.

If it is verified that the cationic charge is preferentially required for antimicrobial PDI, the influence of number and distribution of charges is controversial [38–40]. For example, Reynoso observed that the cationic ammonium group directly attached to the *meso*-phenyl ring of BODIPYs makes PSs more prone to interact with microbial cells than BODIPYs in which positive charge is isolated by an aliphatic spacer [41]. On the contrary, Palacios et al. observed that the aliphatic spacer in the aryl substituent of the two tested BODIPYs provides higher mobility of the charged group which can facilitate the binding of PSs to bacterial cells, increasing its PDI activity [42]. In accordance with Palacios, the two mono-cationic BODIPYs **B14** and **B15**, with charge separated by a spacer, were more prone to bind to microbial cells than **B13** with a cationic charge on phenyl-ring.

As previously highlighted, ideal PSs should not be toxic to microorganisms in dark conditions in order to display their killing effect only upon specific irradiation [4]. Awuah observed that BODIPYs incorporating heavy atoms such as Iodine showed higher intrinsic toxicity compared to

Fig. 4 Confocal microscopy images of *C. albicans* ATCC 14053 cells upon photodynamic treatment with BODIPYs (**B2**, **B5**, **B7**, **B8**, **B12**, **B13**) 10 μM activated by light at 520 nm (20 J/cm^2). Untreated samples and cells treated with 1% DMSO are included. Cells were dark incubated (**a**, **c**, **e**, **g**, **i**, **m**, **o**, **q**) or irradiated (**b**, **d**, **f**, **h**, **l**, **n**, **p**, **r**). A fluorescent BODIPY was used as dye for confocal microscopy analysis trough 63 × objective lens (Scale bar = 10 μm)
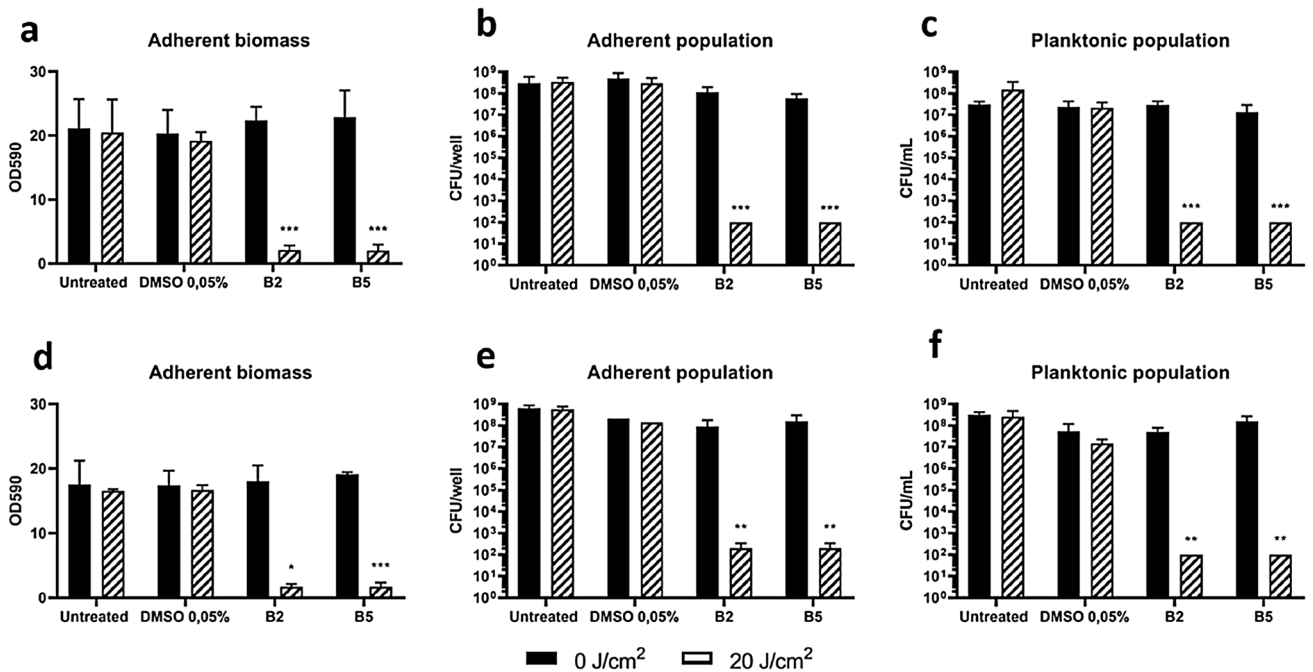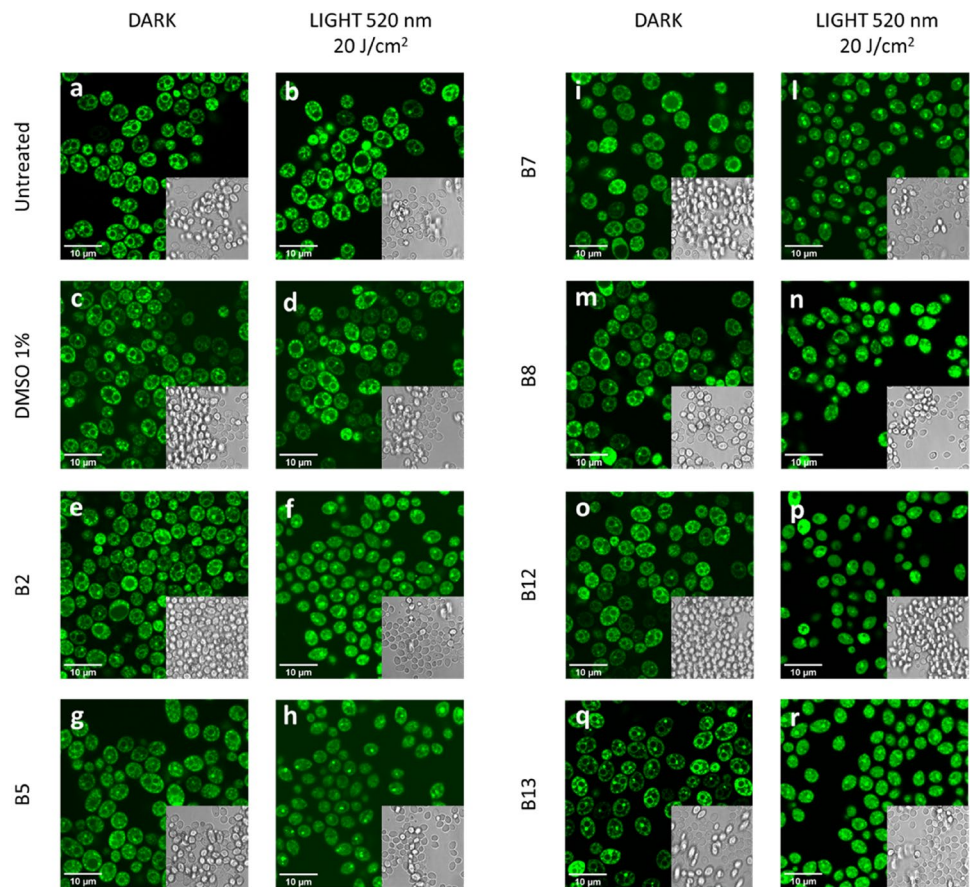

Fig. 5 Inhibition of biofilm formation in *S. aureus* ATCC 6538P (**a**,**b**,**c**) and ATCC 43300 (**d**,**e**,**f**) after photodynamic treatment with BODIPYs **B2** and **B5**. PSs at 0.5 μM concentration were activated by green light at 20 J/cm^2. The graphs report values of adherent biomass (OD590) (**a**, **d**), viability of sessile cells (CFU/well) (**b**, **e**), and viability of planktonic cells (CFU/mL) (**c**, **f**). Dark control samples are presented as black bars and light-treated samples as striped bars. Data represent the mean of at least three independent experiments ± standard deviation. Statistical analyses were performed by one-way ANOVA (*$p < 0.05$; **$p < 0.01$; ***$p < 0.0001$)
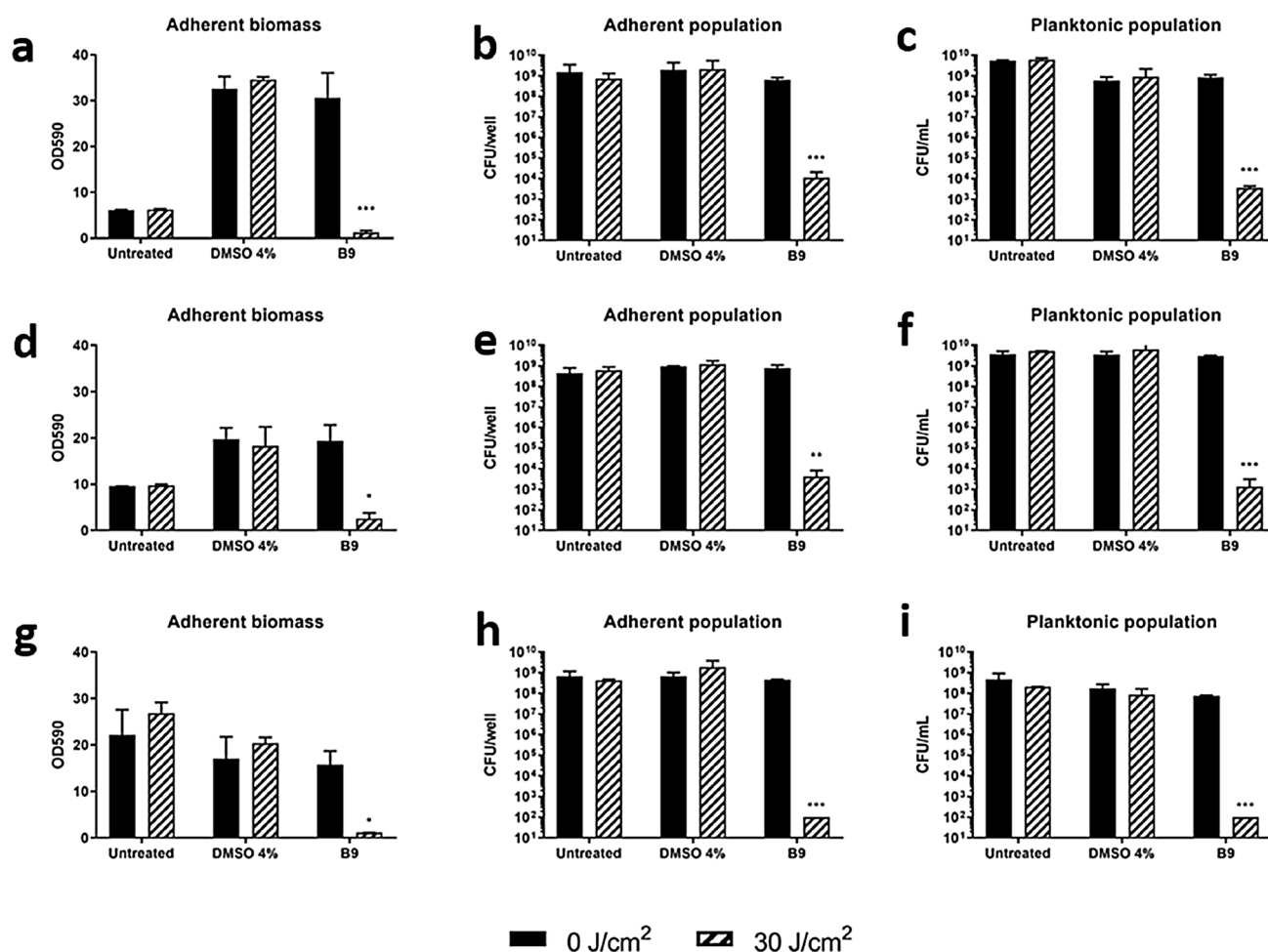
Fig. 6 Inhibition of biofilm formation of *P. aeruginosa* PAO1 (**a**,**b**,**c**), UR48 (**d**,**e**,**f**) and BT1 (**g**,**h**,**i**) strains after photodynamic treatment with **B9**. PS at 40 μM concentration was activated by green light at 30 J/cm² . The graphs report values of adherent biomass (OD 590) (**a**,**d**,**g**), viability of adherent cells (CFU/well) (**b**,**e**,**h**), and viability of planktonic cells (CFU/mL) (**c**,**f**,**i**). Dark control samples are presented as black bars and light-treated samples as striped bars. Data represent the mean of at least three independent experiments ± standard deviation. Statistical analyses were performed by one-way ANOVA (*$p < 0.05$; **$p < 0.01$; ***$p < 0.0001$)

compounds without heavy atoms [12]. Thus, in the iodinated BODIPYs of this study the heavy-atom could play a role. In a study performed on *S. aureus*, Zhao hypothesized that BODIPYs could intercalate into chromosomal DNA [43]. Since we observed that BODIPYs bearing activated aromatic rings were more toxic than those with deactivated rings, further investigations should be performed.

Independently from compound charge, 1 μM PS concentration showed good photoinactivation rates in suspended cultures of *S. aureus*. This was in accordance with results obtained with other classes of PSs, showing that the Gram-positive model was more sensitive than the Gram-negative one [38, 44]. Indeed, *P. aeruginosa* PAO1 resulted the most tolerant to photo-oxidative stress induced by BODIPYs: only the neutral **B9** showed a certain degree of phototoxicity (~ 4 Log unit reduction). PDT-tolerance of *P. aeruginosa* is widely reported, and a possible explanation could be ascribable to the presence of detoxifying enzymes and pigments acting as a defence shield against photooxidative stress, as reported in literature [45–48]. Unexpectedly, in *P. aeruginosa* PAO1, the most active compound was the neutral one **B9** and new similar PSs should be tested to infer further hypotheses on structure–activity relationship. It is noteworthy that in this model strain, the killing rate of BODIPYs was specifically influenced by the experimental setup. Namely, the photoinactivation was more efficient when performed on *P. aeruginosa* cells inoculated on LB agar compared to that on cells suspended in phosphate buffer. Since a potential role as endogenous photosensitizers may be played by cellular porphyrins and flavins, the higher photosensitivity observed in LB medium could be ascribable to an additional effect of bacterial growth [49]. In addition, photoactivable

Fig. 7 Eradication of *P. aeruginosa* PAO1_pVOGFP biofilm. 24-h-old PAO1_pVOGFP biofilm grown on coverslip glass was treated with **B9** at 40 µM concentration and irradiated with light at 520 nm at 30 J/cm^2 or dark incubated. The images represent untreated biofilms (**a,b**), DMSO-treated biofilms (**c,d**) and biofilms treated with **B9** (**e,f**). In each biofilm, planktonic phase was removed and GFP expression was induced by the addition of fresh medium containing arabinose 0.1% W/V. Dark controls are shown in panels a,c,e, irradiated samples in panels b,d,f. Projections and sections of CLSM images of biofilms are shown in volume view. Scale bar = 10 µM
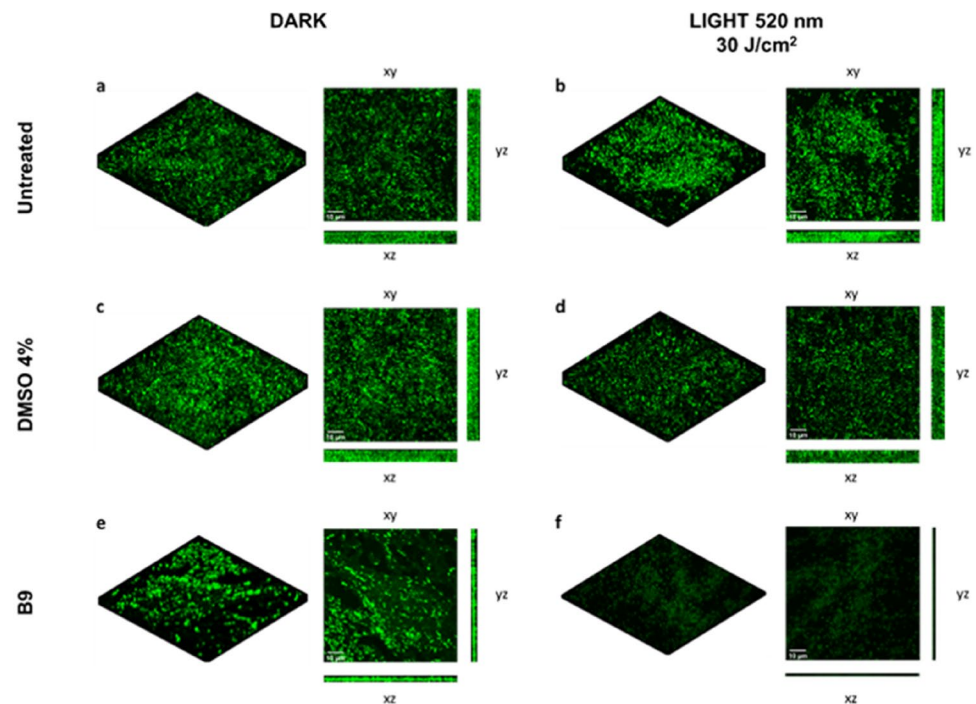
components of LB could play as exogenous PSs and a differential rate of oxygen diffusion should be taken in account, as previously reported by authors for PAO1 strain [34].

The antimicrobial activity of BODIPYs was successfully applied to *C. albicans* suspensions. No intrinsic toxicity was observed and irradiation at a low fluence rate of 20 J/cm^2 resulted in the disappearance of typical compartmentalization.

Antimicrobial PDT has been reported as one of the most promising anti-biofilm strategies [3, 50]. In clinical environments, biofilms are one of the major virulence factors associated with chronic infections and are very difficult to eradicate [51]. Dai et al. obtained very good yields of biofilm photoinactivation with galactose-decorated BODIPYs at 22µM concentration, reaching 80% of eradication of *P. aeruginosa* and *S. aureus* biofilms [52].

In this study, the neutral compounds **B2** and **B5** prevented the development of both planktonic and sessile populations of MSSA and MRSA biofilms*,* regardless of their antibiotic susceptibility profile. Similar results were obtained with natural and neutral compounds curcumin and hypericin [53, 54]. Even if **B2** and **B5** were not able to eradicate 24-h-old biofilms, they greatly compromised the viability of adherent and planktonic cells. It is noteworthy that lower PS concentrations and fluence rates were used to counteract biofilm formation in *S. aureus* as compared to tolerant *P. aeruginosa* strains.

The present screening highlighted the potential of neutral **B9** BODIPY against *P. aeruginosa* biofilms. It was efficient in inhibiting the biofilm formation of PAO1 model strain,

known to be tolerant to antimicrobial treatments and aPDT [55], and also of clinical isolates UR48 and BT1. In this study, when evaluating aPDT effects, a discrimination was made between planktonic and sessile components, while no quantification of extracellular matrix was performed. However, our results could be in agreement with the work of Hendiani et al. that reported a possible involvement of PDT in quorum sensing impairment and inherent matrix production [56].

Non-ionic (**B2**, **B5**, **B7**, **B8**, **B12**) and cationic (**B13**) BODIPYs successfully inhibited the formation of *C. albicans* biofilms, while no activity was observed on formed biofilms. The observed high tolerance of *C. albicans* biofilms to photoinactivation could be in agreement with the reported protective role of matrix in reducing the eradication of *C. albicans* biofilms [57]: as a matter of fact, Garcia et al. observed that *C. albicans* strains with reduced extracellular matrix were sensitive to aPDT [58].

5 Conclusions

From the initial use as fluorescent dyes for imaging and diagnostic purposes, BODIPYs have recently gained increasing attention as photosensitizers in the fight of clinical infections and/or in environmental sanitization. Though cationic compounds, regardless of their chemical structure [59, 60], are considered the best candidates for antimicrobial PDT, this study highlighted neutral BODIPYs as putative pan-photoantimicrobials active against *S. aureus*, *P. aeruginosa* and *C.*
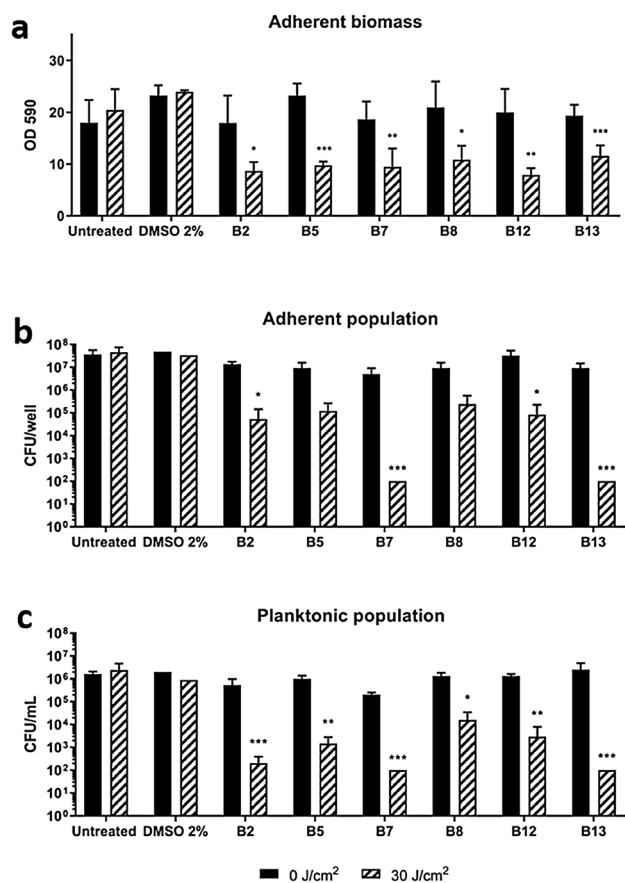
Fig. 8 Inhibition of biofilm formation by *C. albicans* ATCC 14053 upon photodynamic treatment with **B2**, **B5**, **B7**, **B8**, **B12**, **B13**. PSs at 20 μM concentration were activated by light at 520 nm (30 J/cm^2). The graphs report values of the absorbance at 590 nm (OD 590) of biofilm after staining with crystal violet (**a**), values of adherent population viability (CFU/well) (**b**), and planktonic population viability (CFU/mL) (**c**). Dark control samples are presented as black bars and light-treated samples as striped bars. Data represent the mean of at least three independent experiments ± standard deviation. Statistical analyses were performed by one-way ANOVA (*$p < 0.05$; **$p < 0.01$; ***$p < 0.0001$)

albicans. Furthermore, anionic BODIPYs were efficient in inhibiting biofilm formation of all microbial strains.

Supplementary Information The online version contains supplementary material available at https://doi.org/10.1007/s43630-022-00212-4.

Declarations

Conflict of interest The authors report no potential conflict of interest.

References

1. Pendleton, J. N., Gorman, S. P., & Gilmore, B. F. (2013). Clinical relevance of the ESKAPE pathogens. *Expert Review of Anti-Infective Therapy, 11*, 297–308.
2. Roca, I., Akova, M., Baquero, F., Carlet, J., Cavaleri, M., Coenen, S., Cohen, J., Findlay, D., Gyssens, I., Heure, O. E., Kahlmeter, G., Kruse, H., Laxminarayan, R., Liébana, E., López-Cerero, L., MacGowan, A., Martins, M., Rodríguez-Baño, J., Rolain, J. M., … Vila, J. (2015). The global threat of antimicrobial resistance: Science for intervention. *New Microbes New Infect., 6*, 22–29.
3. Mulani, M. S., Kamble, E. E., Kumkar, S. N., Tawre, M. S., & Pardesi, K. R. (2019). Emerging strategies to combat ESKAPE pathogens in the era of antimicrobial resistance: A review. *Frontiers in Microbiology, 10*, 539.
4. Cieplik, F., Deng, D., Crielaard, W., Buchalla, W., Hellwig, E., Al-Ahmad, A., & Maisch, T. (2018). Antimicrobial photodynamic therapy—what we know and what we don't. *Critical Reviews in Microbiology, 44*, 571–589.
5. St Denis, T. G., Dai, T., Izikson, L., Astrakas, C., Anderson, R. R., Hamblin, M. R., & Tegos, G. P. (2011). All you need is light, antimicrobial photoinactivation as an evolving and emerging discovery strategy against infectious disease. *Virulence, 2*, 509–520.
6. Maisch, T. (2015). Resistance in antimicrobial photodynamic inactivation of bacteria. *Photochemical & Photobiological Sciences, 14*, 1518–1526.
7. Hamblin, M. R. (2016). Antimicrobial photodynamic inactivation: A bright new technique to kill resistant microbes. *Current Opinion in Microbiology, 33*, 67–73.
8. Gallagher, W. M., Allen, L. T., O'Shea, C., Kenna, T., Hall, M., Gorman, A., Killoran, J., & O'Shea, D. F. (2005). A potent nonporphyrin class of photodynamic therapeutic agent: Cellular localisation, cytotoxic potential and influence of hypoxia. *British Journal of Cancer, 92*, 1702–1710.
9. Frimannsson, D. O., Grossi, M., Murtagh, J., Paradisi, F., & Oshea, D. F. (2010). Light induced antimicrobial properties of a brominated boron difluoride (BF2) chelated tetraarylazadipyrromethene photosensitizer. *Journal of Medicinal Chemistry, 53*, 7337–7343.
10. Caruso, E., Banfi, S., Barbieri, P., Leva, B., & Orlandi, V. T. (2012). Synthesis and antibacterial activity of novel cationic BODIPY photosensitizers. *Journal of Photochemistry and Photobiology, B: Biology, 114*, 44–51.
11. Agazzi, M. L., Ballatore, M. B., Durantini, A. M., Durantini, E. N., & Tomé, A. C. (2019). BODIPYs in antitumoral and antimicrobial photodynamic therapy: An integrating review. *Journal of Photochemistry and Photobiology, C: Photochemistry Reviews, 40*, 21–48.
12. Awuah, S. G., & You, Y. (2012). Boron dipyrromethene (BODIPY)-based photosensitizers for photodynamic therapy. *RSC Advances, 2*, 11169–11183.

13. Benstead, M., Mehl, G. H., & Boyle, R. W. (2011). 4,4'-Difluoro-4-bora-3a,4a-diaza-s-indacenes (BODIPYs) as components of novel light active materials. *Tetrahedron, 67*, 3573–3601.

14. Gayathri, T., Barui, A. K., Prashanthi, S., Patra, C. R., & Singh, S. P. (2014). Meso-Substituted BODIPY fluorescent probes for cellular bio-imaging and anticancer activity. *RSC Advances, 4*, 47409–47413.

15. Yogo, T., Urano, Y., Ishitsuka, Y., Maniwa, F., & Nagano, T. (2005). Highly efficient and photostable photosensitizer based on BODIPY chromophore. *Journal of the American Chemical Society, 127*, 12162–12163.

16. Durantini, A. M., Heredia, D. A., Durantini, J. E., & Durantini, E. N. (2018). BODIPYs to the rescue: Potential applications in photodynamic inactivation. *European Journal of Medicinal Chemistry, 144*, 651–661.

17. Martínez, S. R., Palacios, Y. B., Heredia, D. A., Aiassa, V., Bartolilla, A., & Durantini, A. M. (2021). Self-sterilizing 3D-printed polylactic acid surfaces coated with a BODIPY photosensitizer. *ACS Applied Materials & Interfaces, 13*, 11597–11608.

18. Cullen, A. A., Rajagopal, A., Heintz, K., Heise, A., Murphy, R., Sazanovich, I. V., Greetham, G. M., Towrie, M., Long, C., Fitzgerald-Hughes, D., & Pryce, M. T. (2021). Exploiting a neutral BODIPY copolymer as an effective agent for photodynamic antimicrobial inactivation. *The Journal of Physical Chemistry B, 125*, 1550–1557.

19. Shao, J., Huang, P. Z., Chen, Q. Y., & Zheng, Q. L. (2020). Nano adamantane-conjugated BODIPY for lipase affinity and light driven antibacterial. *Spectrochimica Acta, Part A: Molecular and Biomolecular Spectroscopy, 234*, 118252.

20. Stoll, K. R., Scholle, F., Zhu, J., Zhang, X., & Ghiladi, R. A. (2019). BODIPY-embedded electrospun materials in antimicrobial photodynamic inactivation. *Photochemical & Photobiological Sciences, 18*, 1923–1932.

21. Zhao, Y., Lu, Z., Dai, X., Wei, X., Yu, Y., Chen, X., Zhang, X., & Li, C. (2018). Glycomimetic-conjugated photosensitizer for specific pseudomonas aeruginosa recognition and targeted photodynamic therapy. *Bioconjugate Chemistry, 29*, 3222–3230.

22. Banfi, S., Nasini, G., Zaza, S., & Caruso, E. (2013). Synthesis and photo-physical properties of a series of BODIPY dyes. *Tetrahedron, 69*, 4845–4856.

23. Caruso, E., Gariboldi, M., Sangion, A., Gramatica, P., & Banfi, S. (2017). Synthesis, photodynamic activity, and quantitative structure-activity relationship modelling of a series of BODIPYs. *Journal of Photochemistry and Photobiology, B: Biology, 167*, 269–281.

24. Caruso, E., Malacarne, M. C., Marras, E., Papa, E., Bertato, L., Banfi, S., & Gariboldi, M. B. (2020). New BODIPYs for photodynamic therapy (PDT): synthesis and activity on human cancer cell lines. *Bioorganic & Medicinal Chemistry, 28*, 115737.

25. Zagami, R., Sortino, G., Caruso, E., Malacarne, M. C., Banfi, S., Patanè, S., Monsù Scolaro, L., & Mazzaglia, A. (2018). Tailored-BODIPY/amphiphilic cyclodextrin nanoassemblies with PDT effectiveness. *Langmuir, 34*, 8639–8651.

26. Klausen, M., Ucuncu, M., & Bradley, M. (2020). Design of photosensitizing agents for targeter antimicrobial photodynamic therapy. *Molecules, 25*(22), 5239.

27. Stover, C. K., Pham, X. Q., Erwin, A. L., Mizoguchi, S. D., Warrener, P., Hickey, M. J., Brinkman, F. S., Hufnagle, W. O., Kowalik, D. J., Lagrou, M., Garber, R. L., Goltry, L., Tolentino, E., Westbrock-Wadman, S., Yuan, Y., Brody, L. L., Coulter, S. N., Folger, K. R., Kas, A., … Olson, M. V. (2000). Complete genome sequence of *Pseudomonas aeruginosa* PAO1, an opportunistic pathogen. *Nature, 406*, 959–964.

28. Orlandi, V. T., Bolognese, F., Rolando, B., Guglielmo, S., Lazzarato, L., & Fruttero, R. (2018). Anti-pseudomonas activity of 3-nitro-4-phenylfuroxan. *Microbiol. (United Kingdom), 164*, 1557–1566.

29. Orlandi, V. T., Martegani, E., Bolognese, F., Trivellin, N., Garzotto, F., & Caruso, E. (2021). Photoinactivation of pseudomonas aeruginosa biofilm by dicationic diaryl-porphyrin. *International Journal of Molecular Sciences, 22*, 6808.

30. Orlandi, V. T., Villa, F., Cavallari, S., Barbieri, P., Banfi, S., Caruso, E., & Clerici, P. (2011). Photodynamic therapy for the eradication of biofilms formed by catheter associated *Pseudomonas aeruginosa* strains. *Microbiologia Medica*. https://doi.org/10.4081/mm.2011.2376

31. Bragonzi, A., Wiehlmann, L., Klockgether, J., Cramer, N., Worlitzsch, D., Döning, G., & Tümmler, B. (2006). Sequence diversity of the mucABD locus in Pseudomonas aeruginosa isolates from patients with cystic fibrosis. *Microbiology, 152*, 3261–3269.

32. Orlandi, V. T., Martegani, E., Bolognese, F., Trivellin, N., Maťátková, O., Paldrychová, M., Baj, A., & Caruso, E. (2020). Photodynamic therapy by diaryl-porphyrins to control the growth of Candida albicans. *Cosmetics, 7*(2), 31.

33. Orlandi, V. T., Martegani, E., & Bolognese, F. (2018). Catalase A is involved in the response to photooxidative stress in *Pseudomonas aeruginosa*. *Photodiagnosis and Photodynamic Therapy, 22*, 233–240.

34. Orlandi, V. T., Rybtke, M., Caruso, E., Banfi, S., Tolker-Nielsen, T., & Barbieri, P. (2014). Antimicrobial and anti-biofilm effect of a novel BODIPY photosensitizer against *Pseudomonas aeruginosa* PAO1. *Biofouling, 30*(8), 883–891.

35. Carpenter, B. L., Situ, X., Scholle, F., Bartelmess, J., Weare, W. W., & Ghiladi, R. A. (2015). Antiviral, antifungal and antibacterial activities of a BODIPY-based photosensitizer. *Molecules, 20*, 10604–10621.

36. Baranzini, N., Monti, L., Vanotti, M., Orlandi, V. T., Bolognese, F., Scaldaferri, D., Girardello, R., Tettamanti, G., De Eguileor, M., Vizioli, J., Acquati, F., & Grimaldi, A. (2019). AIF-1 and RNA-SET2 play complementary roles in the innate immune response of medicinal leech. *Journal of Innate Immunity, 11*, 150–167.

37. Kapteyn, J. C., Montijn, R. C., Dijkgraaf, G. J. P., Van den Ende, H., & Klis, F. M. (1995). Covalent association of β-1,3-glucan with β-1,6-glucosylated mannoproteins in cell walls of Candida albicans. *Journal of Bacteriology, 177*, 3788–3792.

38. Banfi, S., Caruso, E., Buccafurni, L., Battini, V., Zazzaron, S., Barbieri, P., & Orlandi, V. (2006). Antibacterial activity of tetraaryl-porphyrin photosensitizers: An in vitro study on Gram negative and Gram positive bacteria. *Journal of Photochemistry and Photobiology, B: Biology, 85*(1), 28–38.

39. Merchat, M., Spikes, J. D., Bertoloni, G., & Jori, G. (1996). Studies on the mechanism of bacteria photosensitization by meso-substituted cationic porphyrins. *Journal of Photochemistry and Photobiology B: Biology, 35*, 149–157.

40. Caminos, D. A., Spesia, M. B., & Durantini, E. N. (2006). Photodynamic inactivation of *Escherichia coli* by novel meso-substituted porphyrins by 4-(3-N, N, N-trimethylammoniumpropoxy)phenyl and 4-(trifluoromethyl)phenyl groups. *Photochemical & Photobiological Sciences, 5*, 56–65.

41. Reynoso, E., Quiroga, E. D., Agazzi, M. L., Ballatore, M. B., Bertolotti, S. G., & Durantini, E. N. (2017). Photodynamic inactivation of microorganisms sensitized by cationic BODIPY derivatives potentiated by potassium iodide. *Photochemical & Photobiological Sciences, 16*, 1524–1536.

42. Palacios, Y. B., Santamarina, S. C., Durantini, J. E., Durantini, E. N., & Durantini, A. M. (2020). BODIPYs bearing a dimethylaminopropoxy substituent for imaging and photodynamic inactivation of bacteria. *Journal of Photochemistry and Photobiology B: Biology, 212*, 112049.

43. Zhao, C., Zhang, Y., Wang, X., & Cao, J. (2013). Development of BODIPY-based fluorescent DNA intercalating probes. *Journal of Photochemistry and Photobiology, A: Chemistry, 264*, 41–47.

44. Hsieh, C. M., Huang, Y. H., Chen, C. P., Hsieh, B. C., & Tsai, T. (2014). 5-Aminolevulinic acid induced photodynamic inactivation on *Staphylococcus aureus* and *Pseudomonas aeruginosa*. *Journal of Food and Drug Analysis, 22*, 350–355.

45. Orlandi, V. T., Bolognese, F., Chiodaroli, L., Tolker-Nielsen, T., & Barbieri, P. (2015). Pigments influence the tolerance of *Pseudomonas aeruginosa* PAO1 to photodynamically induced oxidative stress. *Microbiology, 161*, 2298–2309.

46. Jornada, D. C., Garcia, R. Q., Silveira, C. H., Misoguti, L., Mendonça, C. R., Santos, R. C. V., Boni, L., & Iglesias, B. A. (2021). Investigation of the triplet excited state and application of cationic meso-tetra(cisplatin)porphyrins in antimicrobial photodynamic therapy. *Photodiagnosis and Photodynamic Therapy, 35*, 1572–1000.

47. Tegos, G. P., Demidova, T. N., Arcila-Lopez, D., Lee, H., Wharton, T., Gali, H., & Hamblin, M. R. (2005). Cationic fullerenes are effective and selective antimicrobial photosensitizers. *Chemistry & Biology, 12*, 1127–1135.

48. Huang, L., Terakawa, M., Zhiyentayev, T., Huang, Y. Y., Sawayama, Y., Jahnke, A., Tegos, G. P., Wharton, T., & Hamblin, M. R. (2010). Innovative cationic fullerenes as broad-spectrum light-activated antimicrobials. *Nanomedicine Nanotechnology Biologie et Médecine, 6*, 442–452.

49. Wang, Y., Wang, Y., Wang, Y., Murray, C. K., Hamblin, M. R., Hooper, D. C., & Dai, T. (2017). Antimicrobial blue light inactivation of pathogenic microbes: State of the art. *Drug Resist. Updat., 33–35*, 1–22.

50. Chanda, W., Joseph, T. P., Wang, W., Padhiar, A. A., & Zhong, M. (2017). The potential management of oral candidiasis using anti-biofilm therapies. *Medical Hypotheses, 106*, 15–18.

51. Jamal, M., Ahmad, W., Andleeb, S., Jalil, F., Imran, M., Nawaz, M. A., Hussain, T., Ali, M., Rafiq, M., & Kamil, M. A. (2018). Bacterial biofilm and associated infections. *Journal of the Chinese Medical Association, 81*, 7–11.

52. Dai, X., Chen, X., Zhao, Y., Yu, Y., Wei, X., Zhang, X., & Li, C. (2018). A water-soluble galactose-decorated cationic photodynamic therapy agent based on bodipy to selectively eliminate biofilm. *Biomacromolecules, 19*, 141–149.

53. Freitas, M. A. A., Pereira, A. H. C., Pinto, J. G., Casas, A., & Ferreira-Strixino, J. (2019). Bacterial viability after antimicrobial photodynamic therapy with curcumin on multiresistant *Staphylococcus aureus*. *Future Microbiology, 14*, 739–748.

54. García, I., Ballesta, S., Gilaberte, Y., Rezusta, A., & Pascual, Á. (2015). Antimicrobial photodynamic activity of hypericin against methicillin-susceptible and resistant *Staphylococcus aureus* biofilms. *Future Microbiology, 10*, 347–356.

55. Azam, M. W., & Khan, A. U. (2019). Updates on the pathogenicity status of *Pseudomonas aeruginosa*. *Drug Discovery Today, 24*, 350–359.

56. Hendiani, S., Rybtke, M. L., Tolker-Nielsen, T., & Kashef, N. (2019). Sub-lethal antimicrobial photodynamic inactivation affects *Pseudomonas aeruginosa* PAO1 quorum sensing and cyclic di-GMP regulatory systems. *Photodiagnosis and Photodynamic Therapy, 27*, 467–473.

57. Cabrini Carmello, J., Alves, F., Basso, F. G., de Souza Costa, C. A., Tedesco, A. C., Lucas Primo, F., de Mima, E. G. O., & Pavarina, A. C. (2019). Antimicrobial photodynamic therapy reduces adhesion capacity and biofilm formation of *Candida albicans* from induced oral candidiasis in mice. *Photodiagnosis and Photodynamic Therapy., 27*, 402–407.

58. Garcia, B. A., Panariello, B. H. D., de Freitas-Pontes, K. M., & Duarte, S. (2021). Candida biofilm matrix as a resistance mechanism against photodynamic therapy. *Photodiagnosis and Photodynamic Therapy., 36*, 102525.

59. Ferreyra, D. D., Reynoso, E., Cordero, P., Spesia, M. B., Alvarez, M. G., Milanesio, M. E., & Durantini, E. N. (2016). Synthesis and properties of 5,10,15,20-tetrakis[4-(3-N, N-dimethylaminopropoxy)phenyl] chlorin as potential broad-spectrum antimicrobial photosensitizers. *Journal of Photochemistry and Photobiology B: Biology, 158*, 243–251.

60. Scanone, A. C., Gsponer, N. S., Alvarez, M. G., & Durantini, E. N. (2018). Porphyrins containing basic aliphatic amino groups as potential broad-spectrum antimicrobial agents. *Photodiagnosis and Photodynamic Therapy, 24*, 220–227.

Authors and Affiliations

Viviana Teresa Orlandi[1] [ORCID] · **Eleonora Martegani[1]** · **Fabrizio Bolognese[1]** · **Enrico Caruso[1]**

✉ Viviana Teresa Orlandi
   viviana.orlandi@uninsubria.it

[1] Department of Biotechnology and Life Sciences, University of Insubria, Via J. H. Dunant, 3, 21100 Varese, Italy